BILINGUAL PUBLISHING CO.
Pioneer of Global Academics Since 1984

Journal of Atmospheric Science Research
https://ojs.bilpublishing.com/index.php/jasr

ARTICLE

Experimental Simulation of Red Sprites in a Laboratory

Victor Tarasenko* **Nikita Vinogradov** **Evgenii Baksht** **Dmitry Sorokin**

Laboratory of Optical Radiations, Institute of High Current Electronics SB RAS, Tomsk, 634055, Russia

ARTICLE INFO

Article history
Received: 30 June 2022
Revised: 20 July 2022
Accepted: 21 July 2022
Published: 30 July 2022

Keywords:
Red sprites
Experimental modeling
Streamer discharge in air
Low pressures

ABSTRACT

Over the past three decades, research of high-altitude atmospheric discharges has received a lot of attention. This paper presents the results of experimental modeling of red sprites during a discharge in low-pressure air. To initiate ionization waves in a quartz tube, an electrodeless pulse-periodic discharge fed by microsecond voltage pulses with an amplitude of a few kilovolts and a repetition rate of tens of kHz were formed. In this case ionization waves (streamers) have a length of tens of centimeters. The main plasma parameters were measured at various distances along the tube. The measurements confirm the fact that ionization waves propagate in opposite directions from the zone of the main electrodeless discharge, just as it happens during the formation of red sprites.

1. Introduction

Much attention is paid to the study of atmospheric discharges. They affect human life, and physical processes occurring in many types of these discharges still require further study. Over the past three decades, many scientific groups have intensively studied Transient Luminous Events (TLEs) such as which include red sprites, blue jets, elves, and others [1-25]. Simulations of TLEs are carried out in laboratory conditions; see for example [4,5]. Figure 1 is a widely known image [10], which presents various types of atmospheric discharges.

One of these types of discharges, which is initiated at altitudes of 70 km ~ 80 km from the Earth's surface and is observed above thunderclouds, are red sprites, see the first color photo [1]. They propagate at altitudes of 40 km ~ 100 km (air pressure varies within 3-2.4·10^{-4} Torr) and their color can change from red to blue one at the altitude of about 50 km. It is known that red sprites can be compared with streamers (ionization waves), which, due to low pressures at high altitudes, have a length of tens of kilometers. It is believed that the red color of sprites is de-

*Corresponding Author:
Victor Tarasenko,
Laboratory of Optical Radiations, Institute of High Current Electronics SB RAS, Tomsk, 634055, Russia;
Email: vft@loi.hcei.tsc.ru

DOI: https://doi.org/10.30564/jasr.v5i3.4858

termined by the emission of bands formed by spectral transitions of the first positive system (FPS; 1+) of a nitrogen molecule [3-6,9,11-13]. Important data on the radiation characteristics of sprites were obtained by observing them from an aircraft [1,23] and from space [6,24]. In particular, a glow duration, emission spectra, and propagation velocities of red sprites were measured and analyzed [1-24]. However, many of the processes that are observed during the formation of red sprites require further research, including in a laboratory. One of such properties of sprites is their propagation both towards the Earth's surface and in the opposite direction [12,17]. The mechanism for initiating red sprites also remains beyond understanding. In particular, it is assumed that their development is initiated by plasma inhomogeneities in the D-region of the ionosphere [25].

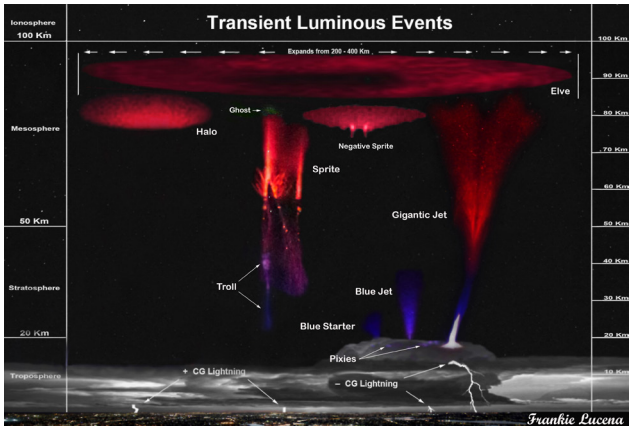

Figure 1. Different types of TLEs. Photo used with permission from F. Lucena [10]

The purpose of this work is to study in details the radiation of a plasma formed by an electrodeless pulse-periodic streamer discharge in air at pressures of 0.4 Torr ~ 9 Torr. Preliminary experiments have shown that such a discharge are red colored due to the emission of bands formed by spectral transitions of the 1+ system of a nitrogen molecule and are can be classified as a streamer discharge. This paper, unlike others dealing with laboratory modeling of red sprites in low-pressure air [15,26-31], has a significant difference in the form of an electrodeless discharge.

2. Experimental Setup and Measuring Techniques

For these studies, a setup was used that had two modifications, which made it possible to study the optical characteristics of a discharge plasma at air pressures corresponding to altitudes where red sprites arise. The setup consisted of a quartz tube (GE 214 grade) with the high transmission in the ultra violet (UV) and visible spectral regions equipped with 1-cm-width ring-shaped electrodes made of aluminum foil, as well as a high-frequency voltage pulse generator (U_g), which was connected to them (Figure 2). A length, an inner diameter and a wall thickness of the tube were 120 cm, 50 mm and 2.5 mm, respectively. The electrodes were located in the center of the tube. A distance between the electrodes was 6 cm.

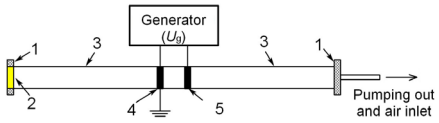

Figure 2. Experimental setup consisting of a quartz tube with ring-shaped electrodes. 1 - flanges; 2 - quartz window; 3 - quartz tube; 4, 5 - ring-shaped electrodes.

In the most experiments, the U_g generator produced voltage pulses with a rise/fall time of ~350 ns, an amplitude of 7 kV, a full width at half-maximum (FWHM) of ≈2 μs. A pulse repetition rate f was 21 kHz. The ends of the tube were closed with caprolon flanges. The right flange had a 5-mm-diameter central hole that served for pumping out and filling the chamber with air A quartz window (2 on Figure 2) or two additional pointed electrodes made of nichrome wire were installed from the side of the left flange (A and C on Figure 3a).

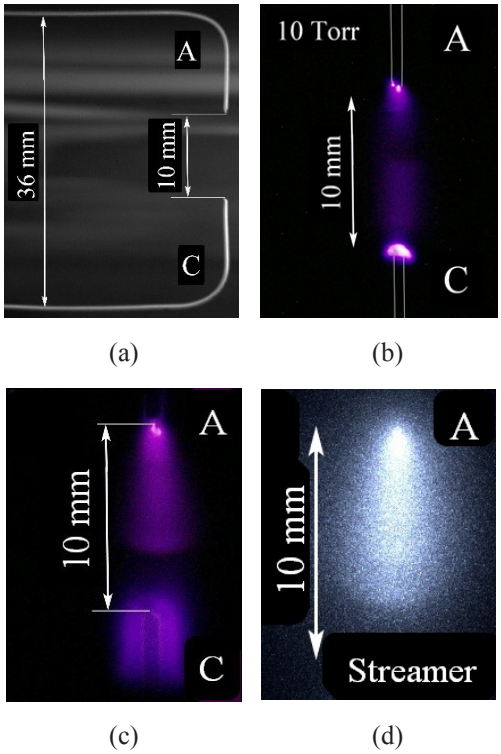

(a) (b)

(c) (d)

Figure 3. Integral photographs of the gap formed by two additional pointed electrodes (A and C) made of 1-mm—diameter nichrome wire (a), discharges without the streamer formation (b) and with it (c), as well as an ICCD image of a streamer (d). Air pressure is p = 10 (b) and 3 Torr (c, d). Amplitude of the voltage applied across the additional pointed electrodes is U_{DC} = +5 kV.

A gap width between the additional electrodes was 10 mm. A radius of curvature of these electrodes was ≈0.1 mm. DC voltage was applied across the additional electrodes from a DC voltage source (U_{DC}) and a discharge was formed at various pressures p and voltages.

The additional electrodes and high-voltage source U_{DC} in a number of cases were used in experiments with the U_g generator and the ring-shaped electrodes. In this case, these electrodes were interconnected outside the chamber and grounded or fed by the U_{DC} source via 100 MΩ resistance. Polarities of the U_g generator and U_{DC} source could change. It was also possible to change the voltage amplitude. Note that the U_{DC} source and additional electrodes are not shown in the Figure 2, however the additional electrodes are shown in the Figure 3a. The voltage across the ring electrodes and the discharge current was measured, correspondingly, by an ACA-6039 (AKTAKOM) voltage divider and a hand-made current shunt. Signals from these probes were recorded with a MDO3104 oscilloscope (Tektronix) with a bandwidth of 1 GHz and a sampling rate of 5 GS/s. The optical characteristics of the discharge plasma radiation were measured with an A100 (SONY) digital camera, an HR2000+ES spectrometer (OceanOptics Inc.) with known spectral sensitivity characteristic, and a four-channel ICCD camera (HSFC-PRO). The HR2000+ES spectrometer (OceanOptics Inc.) allows to record a spectral energy distribution in the range of wavelengths of $\Delta\lambda$ = 190 nm ~ 1100 nm. Its instrumental function is $\Delta\lambda_{instr} \approx 0.9$ nm. In addition, to estimate the main parameters of the formed plasma, an HR4000 spectrometer (OceanOptics Inc.) with known spectral sensitivity characteristic and $\Delta\lambda_{instr} \approx 0.2$ nm was used to record the plasma emission spectrum in the wavelength range $\Delta\lambda$ = 300 nm ~ 400 nm. In experiments with the U_g generator, a streamer velocity was determined with a PD025 photodiode (Photek) with subnanosecond time resolution and the maximum sensitivity in the region of 250 nm ~ 500 nm (LNS20 cathode). Using the photodiode, we recorded the time behavior of the radiation intensity 4-cm-width discharge regions, the centers of which were located at the distance of 3 cm, 13 cm, and 23 cm from the edge of the grounded ring-shaped electrode. The rest of the tube was covered with an opaque screen.

A quartz tube was filled with atmospheric air with a humidity of ≈23%, but first it was pumped out to a residual $p = 10^{-2}$ Torr.

3. Experimental Results

3.1 Characteristics of the Discharge Implemented between Additional Electrodes

The experiment was aimed at determining the influence of the polarity of a high-voltage (HV) electrode on the formation of streamers at low air pressures, as well as fixing their color at pressures of 1 Torr ~ 3 Torr, at which the sprites still remain red. However, the color of the pulsed discharge at low pressures can be either blue or violet [15,26-31]. DC voltage of positive or negative polarity from the U_{DC} source was applied via a 3-m-long cable equipped with a 100-MΩ resistor to the additional electrodes mounted on the left flange (Figure 3a). The bottom electrode in Figure 3a was grounded through the current shunt. In this case, ring-shaped electrodes were not mounted on the tube, and the length of the tube was 20 cm or 120 cm. As experiments have shown, see below, in a number of cases, the length of the tube affected the characteristics of the discharge.

Intense discharge plasma radiation at p = 6 Torr or higher with additional electrodes shown in the Figure 3a was observed only at their tips (Figure 3b). The discharge current and voltage across the gap (less than U_{DC}) were constant during the discharge. Voltage was applied to the additional electrodes via a 100-MΩ-resistance. If there was no breakdown in the tube, the voltage at the electrodes and at the output of the source (U_{DC}) was the same. In the case of air breakdown, a discharge plasma resistance was connected in series with the 100-MΩ-resistance, and the voltage was redistributed between these two resistances in inverse proportion to their values. Accordingly, the voltage across the electrodes decreased. Streamers (ionization waves) usually were not observed under these conditions.

The formation of streamers in a quasi-stationary regime was recorded at p = 1 and 3 Torr with a relatively low U_{DC}. An integral photograph of the discharge plasma glow is shown in Figure 3c. Here we can see the glow near the electrodes and a streamer propagating from the HV anode. An image of a streamer obtained with an ICCD camera under these conditions is shown in Figure 3d. Reducing the frame duration made it possible to register only the streamer glow without stationary plasma radiation at the opposite electrode. The length of streamers arisen under these conditions was less than d, and they were generated in the repetitively pulsed mode. The voltage across the gap in the period between current pulses slowly increased and quickly decreased (the source provided DC voltage). A discharge current waveform had both constant and alternating components (Figure 4).

Under these conditions, the gap breakdown voltage was almost an order of magnitude lower than that supplied from the source. The discharge current was ≈0.65 mA. The repetition rate of the current pulses increased due to increasing U_{DC}. This discharge regime is due to the formation of cylindrical streamers, which do not have time to bridge the gap. Due to the high resistance (100 MΩ), as well as the small capacitance of the interelectrode gap, the voltage across the latter rapidly decreases during the streamer formation process. This leads to the cessation of the development and propagation of a streamer that

has not reached the opposite electrode, as well as to the recombination of a dense streamer plasma in the gap. Accordingly, a pulsed discharge current mode is implemented, in which the current value rapidly increases and then decreases by more than an order of magnitude. The increase in current is due to the charging of the increasing capacitance between the streamer front and the opposite electrode. It was proposed to call dynamic displacement current (DDC) the current flowing through a gap in this mode [32]. The streamer dimensions and its front velocity, as well as the voltage determine the DDC amplitude across the gap. The latter in these experiments, due to the large value of the charging resistance and small interelectrode capacitance, rapidly decreased with increasing conductivity current. This leads to an increase in the plasma resistance after the streamer stops in the gap and the dense plasma recombines. Then, the voltage across the gap increases again. When the threshold voltage is reached, a streamer is formed again. Moreover, at low air pressures, streamers are formed from the positive electrode, and this electrode could be either HV or grounded. At the air pressure of several of Torr, cylindrical streamers near the positive tip begin to form at lower voltage values than at the negative one. An increase in U_{DC}, in this case, will lead to a gap breakdown [33]. The data are in agreement with the results obtained with corona and diffuse discharges from a metal tip [29,34], as well as with an apokampic discharge from a positive charged bent plasma channel between two pointed electrodes [28]. When a pointed electrode is a cathode (a negative tip) electrons move to a region where an electric field strength is lower, i.e. they move away from the cathode tip. There they attach to oxygen molecules. Due to this, the electric field strength at the tip decreases and higher voltage is required to form a streamer. With a positive tip, electrons move to the tip, and positive ions, due to their greater mass, accumulate at the tip and amplify the electric field in this area. This facilitates the formation of a positive cylindrical streamer [29]. As a result, breakdown in an inhomogeneous electric field occurs at a positive polarity of an electrode with a small radius of curvature at a voltage 2-3 times lower than at a negative one (see, e.g., [33]). At nanosecond voltage pulses and low pressures, the color of the discharges was blue or violet [23,26-31] (without taking into account the influence of the interelectrode material [30]). Under the conditions of the experiments, the color of plasma emission both in the region where streamers propagate and in the region near the electrodes was red, including at the air pressure in p = 6 Torr ~ 9 Torr, at which streamers were not observed.

At p = 1 Torr, with a decrease in the length of the quartz tube to 20 cm, red plasma formed not in the short gap (d = 10 mm, Figure 3a) formed by the tips of the additional electrodes, but in the longer gap (d = 36 mm, Figures 3a and 5a) between the parallel wire electrodes. In this case, there was no plasma at the tips and between them in the gap with d = 10 mm (Figure 5a). However, red colored plasma is visible in the gap with d = 36 mm formed by the parallel parts (wires) of the additional electrodes, as well as near these wires. With a decrease in p to 0.1 Torr, a violet colored glow appears near the cathode wire (Figure 5b), although red sprite emission is observed in this pressure range. The purpose of the description of this experiment is to show that discharge modes at low pressures can differ significantly under different conditions. In the future, we plan to study in detail the detected discharge mode.

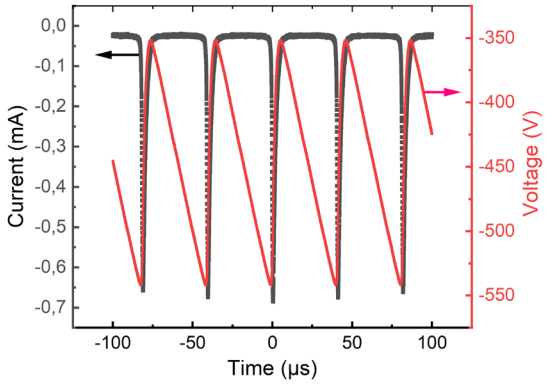

Figure 4. Waveforms of the voltage across the gap and discharge current at the air pressure p = 3 Torr. U_{DC} = +5 kV.

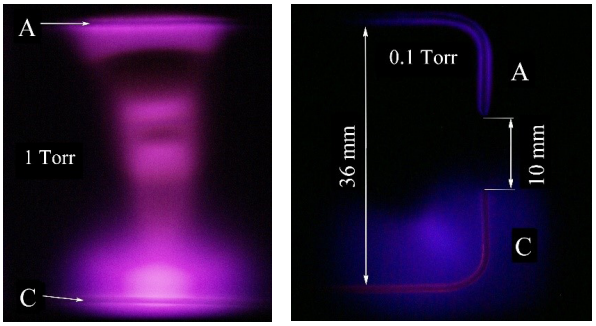

(a) (b)

Figure 5. Integral photographs of the discharge plasma glow in the gap (d = 36 mm) formed by the parallel parts (wires) of the additional electrodes at p = 1 Torr (a) and p = 0.1 Torr (b) in the 20-cm-length tube. U_{DC} = +5 kV.

Thus, the experiment with additional electrodes confirmed that the formation of streamers leading to gap breakdown from a positive polarity electrode with a small radius of curvature occurs at lower voltages than from an electrode of negative polarity. Herewith, this positive electrode can be either HV or grounded.

However, it should be noted, that the formation of red

sprites occurs without metal electrodes. This explains why we used an electrodeless high-frequency discharge between two ring-shaped electrodes (Figure 2).

3.2 Characteristics of the Discharge Implemented between Ring-shaped Electrodes

To provide no plasma contact with electrodes, a repetitively pulsed mode was used. The U_g generator operated at f = 21 kHz provided the formation of a streamer discharge between ring-shaped electrodes mounted on the outer surface of the quartz tube. The main discharge zone was located in the tube center. The distance between the electrodes was d = 6 cm, while their width was 1 cm each. As noted above, the left electrode was grounded, and the right one was HV. The source provided voltage pulses of both positive and negative polarity. The voltage pulse amplitude was U_g = 7 kV. The rise time of voltage pulse t_f and its duration τ (FWHM) were ≈ 350 ns and ≈2 μs, respectively. The experimental setup made it possible to obtain extended streamer discharges at pressures in p = 0.4 Torr ~ 3 Torr. Figure 6 shows photographs of the discharge plasma glow at p = 0.4 Torr with additional electrodes, which were either short circuited or grounded, and without them. In the latter case, a quartz window was installed at the left side of the tube, see Figure 2.

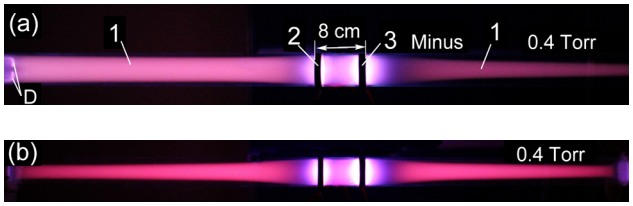

Figure 6. Integral photographs of the electrodeless discharge in the quartz tube (horizontal arrangement) with the additional electrodes (a) and without them (b). p = 0.4 Torr. D - grounded additional electrodes. 1 - ionization waves (streamers), 2 - ring-shaped electrode (grounded), 3 - high voltage (HV) ring-shaped electrode of negative polarity. U_g = 7 kV. Shutter speed 0.05 s, lens aperture f/5.6.

The discharge was initiated in the region characterized by the highest electric field, i.e. between the ring-shaped electrodes and near them. This electrodeless discharge is a capacitive one. The color of the discharge plasma in the tube on both sides of the ring-shaped electrodes was red and depended on whether contact with the additional electrode occurred or not. At p = 0.4 Torr, ionization waves (streamers) reached the left end of the tube. This affected the color of the discharge plasma glow and led to an increase in the transverse dimensions of the discharge region (Figure 6a). A further decrease in p, even without additional electrodes, contributed to the fact that the streamers were in contact with both ends of the tube.

Changing the polarity of the HV ring-shaped electrode (3) did not have a strong effect on the discharge morphology. Integral photos of the discharge plasma glow at p = 1 Torr and both polarities of the HV ring-shaped electrode are shown in Figure 7.

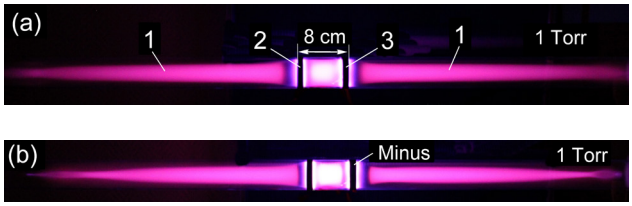

Figure 7. Integral photographs of the discharge plasma glow in the quartz tube without an additional electrode filled with air at p = 1 Torr: positive (a) and negative (b) polarity. U_g = 7 kV. 1 - ionization waves (streamers), 2 - ring-shaped electrode (grounded), 3 - high voltage (HV) ring-shaped electrode of positive polarity. U_g = 7 kV. Shutter speed 0.05 s, lens aperture f/5.6.

As we can see, the morphology and color of the discharge without an additional electrode(s) on the left flange weakly depend on the polarity of the HV ring-shaped electrode. The main differences can be seen at the fronts of the ionization waves, photographs of which are demonstrated in Figure 8.

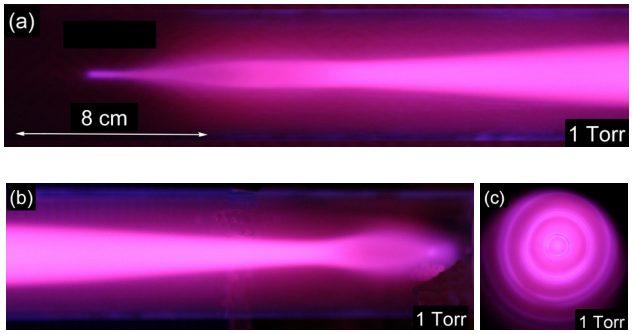

Figure 8. Integral photographs of the discharge plasma glow in the quartz tube (without additional electrodes) to the left (a) and to the right (b) of the ring-shaped electrodes at the positive polarity of the HV electrode, as well as a photograph of the discharge plasma glow (c) captured through the quartz window embedded to the left flange (see Figure 2) at p = 1 Torr. U_g = +7 kV.

The ionization wave on the left side has a pointed end. The photo captured through the quartz window embedded to the left flange shows that there is a bright spot in the center, which, apparently, is due to the emission of a part of the ionization wave with a small diameter near the window (Figure 8a). The color of the discharge regions in all photographs is the same.

A decrease in the amplitude of a voltage pulse pro-

duced by the generator leads to a decrease in the length of an ionization wave on both sides of the ring-shaped electrodes. This is demonstrated in Figures 9a,b,c at air pressure of 1 Torr.

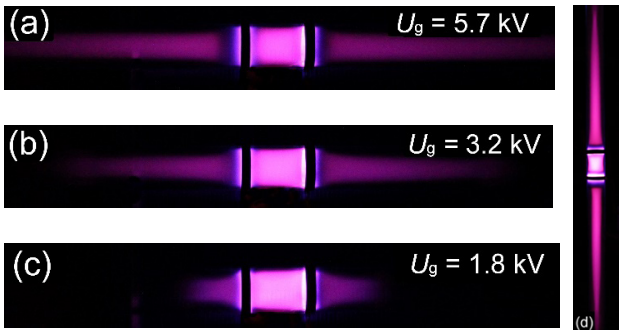

Figure 9. Integral photographs of the discharge plasma glow in the quartz tube (without an additional electrodes) placed horizontally (a, b, c) at various generator voltages and placed vertically at U_g = 7 kV and p = 1 Torr (d). The polarity of the right ring-shaped electrode (a, b, c) and the upper one (d) is positive.

With a decrease in U_g, the length of an ionization wave on the left and right sides of the ring-shaped electrodes decreased, which was to be expected from a decrease in the reduced electric field strength *(U/pd)*. However, the red color of the discharge plasma was preserved. A similar shortening of the streamer length and color preservation were observed with a further increase in p to 3 Torr. At p = 6 Torr and 9 Torr and U_g = 7 kV, a red colored discharge was formed only between the ring-shaped electrodes. There was no discharge in other zones of the quartz tube.

Figures 6 ~ 9a,b,c show the streamer discharge when the quartz tube is placed parallel to the Earth's surface. This position was easy-to-measure of current, voltage, etc. In addition, in a number of experiments, the tube was placed transversely to the Earth's surface (Figure 9d). From the comparison of Figure 7a and Figure 9d, it is seen that the tube position did not affect the formation of ionization waves, as well as their appearance and color. Ionization waves were photographed at the same pressure p = 1 Torr, positive polarity of the high-voltage ring-shaped electrode, and U_g = 7 kV.

The emission spectra of a plasma formed in the region where ionization waves propagate recorded from both sides of the ring electrodes were also the same and did not depend on the position of the quartz tube.

Figure 10 shows the spectral energy distribution W_{spec} obtained from the plasma region located at the distance of 13 cm from the left ring-shaped electrode.

The emission spectra of ionization waves at the distance of several centimeters from the ring-shaped electrodes is similar to those of red sprites [17,18,20,21]. Nitrogen bands belonging to the 2+ and 1+ system contribute predominantly to the spectral energy distribution. Although under these conditions the spectral energy density of radiation of individual bands of the 2+ system exceed that of the 1+ system by more than an order of magnitude, the discharge plasma glow in integral images are red colored (Figures 6 ~ 9). When visually observed, their color is also red.

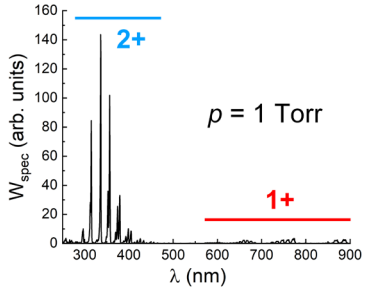

Figure 10. Emission spectrum of the discharge plasma in air at p = 1 Torr recorded at the distance of 13 cm from the left ring-shaped electrode. U_g = +7 kV. 2+ - the second positive system (SPS) of a nitrogen molecule, 1+ - the first positive system (FPS) of a nitrogen molecule.

Figure 11 shows a discharge plasma emission spectrum obtained at the distance of 13 cm from the left ring-shaped electrode at the same air pressure as in Figure 10, but with a light filter (ZhS-12) that cuts off radiation in the wavelength range shorter than 450 nm.

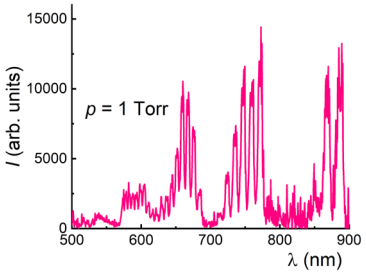

Figure 11. Emission spectrum of air plasma at p = 1 Torr recorded at the distance of 13 cm from the grounded ring-shaped electrode to the left with a light filter (ZhS-12) that cuts off radiation in the wavelength range shorter than 450 nm obtained. U_g = +7 kV.

The use of the filter, which has a transmission of ≈90% in the region of 500 nm ~ 1800 nm and a strong absorption in the region shorter than 450 nm, made it possible to identify the main nitrogen bands belonging to the 1+ system, which coincided with good accuracy with the emission spectra of red sprites [17,18,20,21].

The emission spectra from the ionization wave regions obtained to the right and left of the ring-shaped electrodes (starting from a few centimeters from them) practically

coincide and do not depend on air pressure. The spectra, as we noted before, show, that the radiation of the 2+ system dominates. The spectral energy density of this radiation in individual bands is more than an order of magnitude higher that of the 1+ system. As the pressure increases, the ratio of the intensity of the bands belonging to the 2+ system to the intensity of the bands of the 1+ system can exceed two orders of magnitude. As the pressure decreases to 0.4 Torr, this intensity ratio difference decreases to one order of magnitude. It follows from the data obtained that the emission spectra of ionization waves that propagate in opposite directions are the same. This, as well as their other properties, confirms that it is possible to form two ionization waves from one region, propagating in opposite directions.

Figure 12 shows the spectrum recorded at lower air pressure from the region of an enhanced electric field near the ring electrodes and between them. It is seen, that the spectral energy density of radiation of the first negative band (1-) of a nitrogen molecular ion increases significantly. Wherein, the spectral energy density of their individual lines can be the highest. So, in the area between the electrodes at p = 0.4 Torr, the most spectral radiation energy density at U_g = 7 kV had an ion line of the nitrogen molecule with a wavelength of 391.4 nm (Figure 12). This is explained by an increase in the reduced electric field strength E/N (E is the electric field, N is the concentration of air particles) in this region. The radiation spectrum of dark areas in electrodes (see, e.g., Figure 6) was similar to that in Figure 12 and at p = 1 Torr. Herewith, the width of the dark areas decreased with increasing p. This indicates an increase in the average electron energy. As can be seen from the images in Figure 6, the color in these areas changes. On the other hand, the radiation spectrum of an ionization wave at p = 0.4 Torr at the distance of 10 cm and more from the right ring-shaped electrode was similar to that in Figure 10.

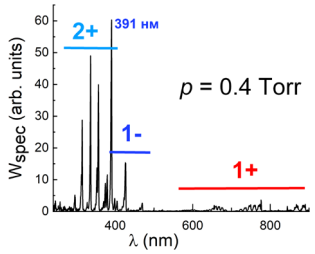

Figure 12. Emission spectrum of the discharge plasma glow from the region between the ring-shaped electrodes. 2+ - the second positive system of a nitrogen molecule, 1+ - the first positive system of a nitrogen molecule, 1- - the first negative system of a nitrogen molecular ion. U_g = 7 kV. Air, p = 0.4 Torr.

Red colored glow regions, which are directed in opposite directions from the main capacitive discharge between the ring-shaped electrodes, are formed due to the propagation of ionization waves. This is confirmed by measurements of the main parameters of the discharge plasma along the tube. The main parameters of the plasma formed at the air pressure in the tube of 1 Torr were measured with optical emission spectroscopy (OES) methods [35-38]. We used plasma emission spectra recorded from the middle part of the tube (the middle of the distance between the inner edges of the ring-shaped electrodes), as well as at distances of 3 cm, 13 cm, and 23 cm to the right and left of the outer edge of the electrodes. First of all, using a method based on measuring the ratio of the peak intensities of the ion (391.4 nm) and molecular (394.3 nm) nitrogen bands [35,36], we estimated the integral values of the electron temperature T_e and the reduced electric field strength E/N. The measurements show that an increase in the distance from the central part of the tube leads to a change in these values from 4.5 eV to 2.5 eV and from 600 Td to 350 Td (which is still quite high), respectively, which is characterized by a relatively small change in the ionization wave front velocity (see the measurement results below). The vibrational temperature T_v and the gas temperature T_g were also estimated by applying the Boltzmann method [36,38,39] to the emission spectra of the discharge plasma. We would also like to note that these temperatures are practically unchanged over the entire length of the tube and their average values are ~2700 and ~380 K, respectively. The reliability of the given values is confirmed by modeling the emission spectra of the plasma using the SPECAIR code [40], where these values are used as input data. Despite the fact that the experimentally measured values of the main parameters make it possible to obtain an almost complete coincidence of the simulated spectral distribution of the radiation energy with the emission spectrum recorded by the HR4000 spectrometer, a feature associated with the discharge morphology appears during the simulation. Thus, the simulation data show some increase in the electron density with increasing distance to the tube ends. At a distance of 1 cm from electrode, the electron density was ~$4 \cdot 10^{11}$ cm^{-3}, and at a distance of 23 cm it became ~$2 \cdot 10^{12}$ cm^{-3}. As follows from Figures 6, 7 and 9, the diameter of the ionization waves (streamers) decreases with distance from the electrodes in both directions. The area of the ionization wave increases in proportion to the square of it diameter. The discharge current in part of ionization wave does not decrease significantly and the current density increases. Although the plasma parameters for air pressures below 1 Torr have not been estimated for this case, it can be confidently claimed

that T_e and *E/N* should be much higher in this case. This is confirmed by the large values of the peak intensity of the nitrogen molecular ion band relative to the intensity of the molecular band (see Figure 12).

Evidence for the implementation of the streamer discharge regime outside the ring-shaped electrodes is also high plasma velocities at various distances from the region where the discharge is initiated. The measurements were carried out using a photodiode. The calculations showed that the average velocity of the glow front between the first (3 cm from the grounded ring-shaped electrode, Figure 6) and the second (13 cm) points was 0.17 cm/ns, and between the second and third ones (13 cm and 23 cm) was 0.12 cm /ns. These values correspond to the propagation velocities of streamers at low pressures [12,41,42] and red sprites [12,17,21,43-45]. During measurements with the photodiode, the bands of the 2+ nitrogen system was mainly recorded. The radiation energy density in individual bands of the 2+ system (UV region, Figure 10) is significantly greater than that for 1+ bands. In addition, the lifetime of the upper level $C^3\Pi_g$ of a nitrogen molecule is more than an order of magnitude shorter than that of $B^3\Pi_g$. The photodiode also had the highest sensitivity in the UV region of the spectrum.

4. Discussion

When comparing the results obtained in the laboratory and those recorded during observations of red sprites, the following important point should be taken into account. The pressure at altitudes where red sprites propagate varies from $2.5 \cdot 10^{-4}$ Torr (100 km) to ≈0.8 Torr (50 km). At the same time, when the altitude changes from 55 km ($p \approx$ 0.4 Torr) to 55.3 km ($p \approx 0.42$ Torr) relative to the Earth's surface, the pressure increases by only 5%. Therefore, the streamer front propagates a few meters at almost constant pressure *p* and particle concentration *N*. Based on this fact, we can assume that the change in air pressure at different altitudes should not lead to significant differences in the properties of the ionization wave in the laboratory and red sprites when moving over short distances. Their velocities, color, as well as emission spectra should be similar. The studies carried out confirm this conclusion. Table 1 shows the main properties of red sprites and ionization waves, which were obtained in our studies. You can see their correspondence.

Let us analyze the obtained results again, compare them with the known data on the development of red sprites, and propose a model for the sprites formation. In experiments, we observed the formation of ionization waves from the plasma of a capacitive discharge. For the formation of red sprites, it is also necessary to have a plasma with a sufficiently high concentration of electrons and ions. We assume that diffuse discharges between different areas of noctilucent clouds are the source of the preliminary plasma. It is known that noctilucent clouds are formed approximately at the same altitudes as red sprites occur [46]. The charge separation in noctilucent clouds, which may consist of ice crystals, occurs similarly to the separation of charges in thunderclouds near the Earth's surface [47]. During diffuse discharges, plasma has a relatively low radiation intensity due to low air pressure at high altitudes. Therefore, this radiation has not yet been experimentally detected. We assume that in a number of cases diffuse discharges in noctilucent clouds at a sufficient value of the reduced electric field *E/N* initiates the formation of ionization waves - sprites. However, we do not deny the possibility of the appearance plasma inhomogeneities and red sprites in the D-region of the ionosphere [25].

The direction of downward sprites at the first stage generates the electric field, which should be directed from appearing place to the negative charge surface. This may be the Earth's surface or the upper surface of thunderclouds. Although, the latter usually has a positive charge [3,4,13,47], but during cloud-to-ground lightning from the upper layer of clouds, the negative charge of the Earth is transferred to this region. As follows from the experiments, the length of the left ionization wave increases when a negative voltage is applied to the additional electrode or when it is grounded (Figure 6a). When sprites that are directed downwards are formed, their length, in addition to reducing the electric field, limits the increase in gas pressure at large distances. It should also be taken into account that the magnitude of the electric field above thunderclouds

Table 1. Comparative characteristics of sprites and ionization waves.

Research object	Color	Main spectral bands	Front velocity, m/s	Pressure, Torr	Electron temperature, eV	Reduced electric field strength, Td	Refs.
Sprite	Red	FPS (1+); SPS; (2+)	$(0.4\text{-}1.7) \cdot 10^7$	$(3\text{-}2.4) \cdot 10^{-4}$	1-2	1s-1000s Td	[4,12,20-22, et al.]
Ionization wave	Red	FPS (1+); SPS; (2+)	$(1.2\text{-}1.7) \cdot 10^7$	3-0.4	≈2.5	≈350 Td	This paper

changes due to the presence of lightning and the development of the sprite. Apparently, a change in the electric field leads to the propagation of red sprites upward from the Earth's surface, and can also lead to the propagation of sprites in different directions [17,18,22,41]. The observed chaotic direction of sprites at altitudes of about 70 km ~ 80 km can also be explained by the uneven distribution of charges in the region of noctilucent clouds.

5. Conclusions

It was shown that using a high-frequency electrodeless discharge, it is possible to simulate the properties of red sprites in a laboratory. This possibility was achieved by recording the integral radiation of tens of thousands of individual pulses. At the air pressure of ≈1 Torr or less, the radiation intensity of the streamer discharge plasma with centimeter dimensions is low. Registration of red sprites in the Earth's atmosphere is simple due to their large size. Using the methods of formation of streamer discharges, a plasma formation with a length of more than 1 m was realized with properties corresponding to those in the plasma of discharges occurring in the natural environment. The air pressure range, observed emission spectra, velocities of ionization wave propagation, as well as visually observed and imprinted color of the discharge plasma glow confirm this. Thus, the length of ionization waves in free space reached 50 cm and was limited by the size of the chamber used as the pressure decreased. As in the sprites, bands 1+ and 2+ systems of a nitrogen molecule dominate in the emission spectrum of the discharge plasma. Moreover, the spectral energy density of the bands of the 2+ system on individual lines was greater than that of the most intense emission bands of the 1+ system. The velocity of ionization wave under laboratory conditions reached 2 mm/ns, which also agrees with the sprite front velocity [12,17,43-45]. The color of the generated ionization waves in a wide range of experimental conditions at appropriate pressures was red, as in sprites. In addition, the paper shows the possibility of generating two streamers that propagate in two opposite directions from a diffuse electrodeless plasma of a capacitive discharge.

Author Contributions

VT supervised the project, analyzed the results, and wrote the manuscript. EB and NV carried out the experiments. DS analyzed the results and performed simulations.

Conflict of Interest

The authors declare that the research was conducted in the absence of any commercial or financial relationships that could be construed as a potential conflict of interest.

Funding

The study is funded by the Ministry of Science and Higher Education of the Russian Federation within Agreement no. 075-15-2021-1026 of November 15, 2021.

Acknowledgments

The authors are thankful to G.V. Naidis for the helpful discussion and to D.S. Pechenitsin for the development and creation of the pulse generator with a high repetition rate.

References

[1] Sentman, D.D., Wescott, E.M., Osborne, et al., 1995. Preliminary results from the Sprites94 aircraft campaign: 1. Red sprites. Geophysical Research Letters. 22(10), 1205-1208.

[2] Bell, T.F., Reising, S.C., Inan, U.S., 1998. Intense continuing currents following positive cloud-to-ground lightning associated with red sprites. Geophysical Research Letters. 25(8), 1285-1288.

[3] Pasko V.P., 2007. Red sprite discharges in the atmosphere at high altitude: the molecular physics and the similarity with laboratory discharges. Plasma Sources Science and Technology. 16. S13.
DOI: https://doi.org/10.1088/0963-0252/16/1/S02

[4] Rodger, C.J., 1999. Red sprites, upward lightning, and VLF perturbations. Reviews of Geophysics. 37(3), 317-336.

[5] Raizer, Y.P., Milikh, G.M., Shneider, M.N., 2010. Streamer-and leader-like processes in the upper atmosphere: Models of red sprites and blue jets. Journal of Geophysical Research: Space Physics. 115, A7.
DOI: https://doi.org/10.1029/2009JA014645

[6] Neubert, T., Østgaard, N., Reglero, V., et al., 2019. The ASIM mission on the international space station. Space Science Reviews. 215(2), 1-17.
DOI: https://doi.org/10.1007/s11214-019-0592-z

[7] Wang, Y., Lu, G., Ma, M., et al., 2019. Triangulation of red sprites observed above a mesoscale convective system in North China. Earth and Planetary Physics. 3(2), 111-125.
DOI: https://doi.org/10.26464/epp2019015

[8] Jiang, F., Huang, C., Wang, Y., 2019. Emission spectrum of sprites caused by the quasi-electrostatic field above thunderstorm clouds. Meteorology and Atmospheric Physics. 131(3), 421-430.

DOI: https://doi.org/10.1007/s00703-018-0579-4

[9] Kuo, C.L., Williams, E., Adachi, T., et al., 2021. Experimental Validation of N2 Emission Ratios in Altitude Profiles of Observed Sprites. Frontiers in Earth Science. 9, 1102.
DOI: https://doi.org/10.3389/feart.2021.687989

[10] Facebook. Available online: http://www.facebook.com/frankie.lucena.1 (Accessed on 01.11.2021).

[11] Füllekrug, M., Mareev, E.A., Rycroft, M.J., (Eds.), 2006. Sprites, elves and intense lightning discharges. Springer Science & Business Media. V. 225.

[12] Kanmae, T., Stenbaek-Nielsen, H.C., McHarg, M.G., et al., 2012. Diameter-speed relation of sprite streamers. Journal of Physics D: Applied Physics. 45(27), 275203.
DOI: https://doi.org/10.1088/0022-3727/45/27/275203

[13] Ebert, U., Nijdam, S., Li, C., et al., 2010. Review of recent results on streamer discharges and discussion of their relevance for sprites and lightning. Journal of Geophysical Research: Space Physics. 115, A00E43.
DOI: https://doi.org/10.1029/2009JA014867

[14] Wang, Y., Lu, G., Cummer, S.A., et al., 2021. Ground observation of negative sprites over a tropical thunderstorm as the embryo of Hurricane Harvey (2017). Geophysical Research Letters. 48(14), e2021GL094032.
DOI:https://doi.org/e2021GL094032

[15] Williams, E.R., 2001. Sprites, elves and glow discharge tubes. Physics Today. 54(11), 41-47.

[16] Huang, A., Lu, G., Yue, J., et al., 2018. Observations of red sprites above Hurricane Matthew. Geophysical Research Letters. 45(23), 13-158.
DOI: https://doi.org/10.1029/2018GL079576

[17] Stenbaek-Nielsen, H.C., McHarg, M.G., 2008. High time-resolution sprite imaging: observations and implications. Journal of Physics D: Applied Physics. 41(23), 234009.
DOI: https://doi.org/10.1088/0022-3727/41/23/234009

[18] Marshall, R.A., Inan, U.S., 2007. Possible direct cloud-to-ionosphere current evidenced by sprite-initiated secondary TLEs. Geophysical research letters. 34(5).
DOI: https://doi.org/10.1029/2006GL028511

[19] Kuo, C.L., Huang, T.Y., Hsu, C.M., et al., 2021. Resolving elve, halo and sprite halo images at 10,000 Fps in the Taiwan 2020 campaign. Atmosphere. 12(8), 1000.
DOI: https://doi.org/10.3390/atmos12081000

[20] Kanmae, T., Stenbaek-Nielsen, H.C., McHarg, M.G., 2007. Altitude resolved sprite spectra with 3 ms temporal resolution. Geophysical Research Letters. 34(7), L07810.
DOI: https://doi.org/10.1029/2006GL028608

[21] Gordillo-Va´zquez, F.J., Luque, A., Simek, M., 2012. Near infrared and ultraviolet spectra of TLEs. Journal of Geophysical Research. 117, A05329.
DOI: https://doi.org/10.1029/2012JA017516

[22] Qin, J., Celestin, S., Pasko, V.P., 2012. Formation of single and double-headed streamers in sprite-halo events. Geophysical Research Letters. 39, L05810.
DOI: https://doi.org/10.1029/2012GL051088

[23] Sentman, D.D., Wescott, E.M., 1993. Observations of upper atmospheric optical flashes recorded from an aircraft. Geophysical Research Letters. 20(24), 2857-2860.

[24] Garipov, G.K., Khrenov, B.A., Klimov, P.A., et al., 2013. Global transients in ultraviolet and red-infrared ranges from data of Universitetsky-Tatiana-2 satellite. Journal of Geophysical Research: Atmospheres. 118(2), 370-379.
DOI: https://doi.org/10.1029/2012JD017501

[25] Qin, J., Pasko, V.P., McHarg, M.G., et al., 2014. Plasma irregularities in the D-region ionosphere in association with sprite streamer initiation. Nature communications. 5(1), 1-6.
DOI: https://doi.org/10.1038/ncomms4740

[26] Anikin, N.B., Zavialova, N.A., Starikovskaia, S.M., et al., 2008. Nanosecond-discharge development in long tubes. IEEE Transactions on Plasma Science. 36(4), 902-903.
DOI: https://doi.org/10.1109/TPS.2008.924504

[27] Tarasenko, V.F., Sosnin, E.A., Skakun, V.S., et al., 2017. Dynamics of apokamp-type atmospheric pressure plasma jets initiated in air by a repetitive pulsed discharge. Physics of Plasmas. 24(4), 043514.
DOI: https://doi.org/10.1063/1.4981385

[28] Sosnin, E.A., Babaeva, N.Y., Kozhevnikov, et al., 2021. Modeling of transient luminous events in Earth's middle atmosphere with apokamp discharge. Physics-Uspekhi. 64(2), 191-210.
DOI: https://doi.org/10.3367/UFNe.2020.03.038735

[29] Tarasenko, V., Baksht, E., Kuznetsov, V., et al., 2020. Corona with Streamers in Atmospheric Pressure Air in a Highly Inho-mogeneous Electric Field. Journal of Atmospheric Science Research. 03(4), 28–37.
DOI: https://doi.org/10.30564/jasr.v3i4.2342

[30] Tarasenko, V., Vinogradov, N., Beloplotov, D., et al., 2022. Influence of Nanoparticles and Metal Vapors on the Color of Laboratory and Atmospheric Discharges. Nanomaterials. 12(4), 652.
DOI: https://doi.org/10.3390/nano12040652

[31] Tarasenko, V.F., 2022. Analysis of Dynamics of At-

mospheric Discharges Using Data on Cylindrically and Spherically Shaped Streamers. Atmospheric and Oceanic Optics. 35(2), 164-167.
DOI: https://doi.org/10.1134/S1024856022020154

[32] Shao, T., Tarasenko, V.F., Zhang, C., et al., 2013. Application of dynamic displacement current for diagnostics of subnanosecond breakdowns in an inhomogeneous electric field. Review of Scientific Instruments. 84(5), 053506.
DOI: https://doi.org/10.1063/1.4807154

[33] Raizer, Y.P., Allen, J.E., 1991. Gas discharge physics. Springer: Berlin.

[34] Tarasenko, V., Beloplotov, D., Burachenko, A., et al., 2020. On the Formation of a Bead Structure of Spark Channels during a Discharge in Air at Atmospheric Pressure. Journal of Atmospheric Science Research. 3(1), 1-8.
DOI: https://ojs.bilpublishing.com/index.php/jasr

[35] Nassar, H., Pellerin, S., Musiol, K., et al., 2004. N2+/N2 ratio and temperature measurements based on the first negative N2+ and second positive N2 overlapped molecular emission spectra. Journal of Physics D: Applied Physics. 37(14), 1904-1916.
DOI: https://doi.org/10.1088/0022-3727/37/14/005

[36] Britun, N., Gaillard, M., Ricard, A., et al., 2007. Determination of the vibrational, rotational and electron temperatures in N2 and Ar–N2 rf discharge. Journal of Physics D: Applied Physics. 40(4), 1022-1029.
DOI: https://doi.org/10.1088/0022-3727/40/4/016

[37] Paris, P., Aints, M., Valk, F., et al., 2005. Intensity ratio of spectral bands of nitrogen as a measure of electric field strength in plasmas. Journal of Physics D: Applied Physics. 38(21), 3894-3899.
DOI: https://doi.org/10.1088/0022-3727/38/21/010

[38] Ochkin, V.N., 2009. Spectroscopy of low temperature plasma. John Wiley & Sons.

[39] Phillips, D.M., 1976. Determination of gas temperature from unresolved bands in the spectrum from a nitrogen discharge. Journal of Physics D: Applied Physics. 9(3), 507-521.

[40] Laux, C.O., 2002. Physico-chemical modeling of high enthalpy and plasma flows. Lecture Series. Belgium: Rhode Saint Genèse.

[41] Sentman, D.D., Stenbaek-Nielsen, H.C., McHarg, M.G., et al., 2008. Plasma chemistry of sprite streamers. Journal of Geophysical Research: Atmospheres. 113, D11112.
DOI: https://doi.org/10.1029/2007JD008941

[42] Liu, N., Pasko, V.P., 2006. Effects of photoionization on similarity properties of streamers at various pressures in air. Journal of Physics D: Applied Physics. 39(2), 327-334.
DOI: https://doi.org/10.1088/0022-3727/39/2/013

[43] Stanley, M., Krehbiel, P., Brook, M., et al., 1999. High speed video of initial sprite development. Geophysical Research Letters. 26(20), 3201-3204.

[44] Cummer, S.A., Jaugey, N.C., Li, J.B., et al., 2006. Submillisecond imaging of sprite development and structure. Geophysical Research Letters. 33, L04104.
DOI: https://doi.org/10.1029/2005GL024969

[45] McHarg, M.G., Stenbaek-Nielsen, H.C., Kammae, T., 2007. Observations of streamer formation in sprites. Geophysical Research Letters. 34(6), L06804.
DOI: https://doi.org/10.1029/2006GL027

[46] Hervig, M., Thompson, R.E., McHugh, M., et al., 2001. First confirmation that water ice is the primary component of polar mesospheric clouds. Geophysical Research Letters. 28(6), 971-974.

[47] Bazelyan, E.M., Raizer, Y.P., 2000. Lightning physics and lightning protection, CRC Press: USA (2001, Fizmatizdat: Moscow, pp. 320).